Energy-transfer processes during Xe^{30+}-Ar collisions for projectile velocities between 0.3 and 1.0 a.u.

M. L. A. Raphaelian, M. P. Stöckli, W. Wu, and C. L. Cocke
Department of Physics, J. R. Macdonald Laboratory, Kansas State University, Manhattan, Kansas 66506-2604
(Received 8 September 1994)

Electron capture by Xe^{30+} from Ar has been studied for projectile velocities between 0.3 and 1.0 a.u. Coincidence measurements were used to identify experimentally the final states of both target and projectile. The capture of up to eight electrons from the target was observed, while retention of more than three electrons by the projectile was found to be rare. Longitudinal recoil momentum spectroscopy was used to determine average Q values for the capture process as a function of recoil charge state. The Q values were found to have no measurable dependence on projectile velocity and were found to be in good agreement with those values predicted by the extended overbarrier model. Relative cross sections for the different final channels were measured and found to be in adequate agreement with the model prediction. A slight increase with increasing projectile velocity in the radiative-stabilization probability for the two-electron states finally formed on the projectile was observed.

PACS number(s): 34.50.Fa, 34.70.+e, 32.80.Dz

I. INTRODUCTION

During the collision between a slowly moving highly ionized heavy projectile and a multielectron target atom, multielectron transfer occurs between the target and the projectile. During this collision process, electrons are shared by both the projectile and target, thereby creating a molecular ion. After the collision, these once shared electrons can be found to be in one of four places: captured by the projectile, recaptured by the target, or located in either the target or projectile continuum. The latter two cases can occur either by Auger processes or by direct ionization processes which occur from electron-electron or electron-nuclear interactions. For the electrons transferred to the projectile, their distribution can lead to their emission into the projectile continuum. Unless one measures the entire emitted electron and photon flux, the total energy carried away from the projectile and recoil, the total change in electronic energy, the Q value of the reaction cannot be deduced from the yield of secondary products. It can be obtained from the loss or gain of translational energy of the projectile [1–16]. The average Q value of the reaction can also be measured by recoil ion longitudinal momentum spectroscopy [15,17–20]. Although the technique does not reveal any structure within the final state distribution, as is often seen for single capture in energy gain measurements, it is easily applied to multiple-electron capture, for which little resolvable structure is expected. In this work, we present the study of the velocity dependence of average Q values obtained using recoil ion longitudinal momentum spectroscopy for single-electron and multielectron transfer during the collision of Xe^{30+} on argon target atoms, and the velocity dependence of the relative cross sections of the different recoil ion production channels. We show that even though the target loses up to eight electrons and the projectile retains up to three electrons, the average Q value for the reaction can be obtained with this technique. We also show that two-electron retention by the projectile increases with increasing collisional velocity within a single recoil-charge species.

To describe multielectron transfer between a highly-charged projectile and a many-electron target atom, the classical barrier model is frequently used [21–23]. The reason why classical and not quantum models are used to describe the collision process is that the number of basis vectors needed in such a quantum calculation is generally unrealistically large for the computational resources available. Classical barrier models involve the independent electron approximation and therefore, apart from screening contributions, electron-electron correlation effects are not taken into account. Specifically the molecular classical "extended" overbarrier model (MCBM) of Niehaus [23] allows for the description of which principal quantum number levels are populated on the projectile during the capture process and, therefore, the energy gain during the collision. The MCBM also gives an estimate of the total single-electron and multielectron capture cross sections and differential cross sections. The overbarrier model of Niehaus, however, does not incorporate any velocity dependence in the capture cross section or predict the angular momentum distribution of the captured electrons. As the collisional velocity increases, higher angular momentum states are observed to be populated [24,25]. An attempt to include velocity dependent effects in the MCBM was proposed and compared with experiments involving helium targets [26]. Comparison of the predictions of the MCBM with experiment have been verified for low velocity collisions [27], typically a few tenths of an a.u. in velocity. Comparison of the predictions from the MCBM for multielectron targets at collisional velocities approaching 1.0 a.u. and for extremely high projectile charge (30+) have not been performed until now.

1050-2947/95/51(2)/1304(8)/$06.00

For a collision involving the transfer of n target electrons into multiexcited states in the projectile, the Q value is defined as the change in electronic energy. The relation between the Q value of the reaction and the momentum transferred during the collision can be derived from conservation of momentum and energy of the collision. For small scattering angles, it leads to

$$Q = -(P_{r_\parallel} v_p + n\tfrac{m_e v_p^2}{2}) + \tfrac{m_p+m_r}{2m_p m_r} P_{r_\perp}^2 + \tfrac{1}{2m_r} P_{r_\parallel}^2, \quad (1.1)$$

where $P_{r_\parallel}$ and $P_{r_\perp}$ are the longitudinal and transverse components of the momentum transferred to the recoil to the beam direction, m_p, m_r, and m_e are the projectile, recoil and electron masses, and v_p is the projectile velocity [20]. The $n(m_e v_p^2/2)$ term is due to the translational kinetic energy that the n electrons must acquire to be captured into the projectile moving frame. At the collisional velocities studied in this experiment the projectile velocity, v_p, is much greater than the transverse velocity component, $v_{r_\perp} = P_{r_\perp}/m_r$, and the Q is dominated by the first two terms in the above equation. Therefore, the energy transferred to the projectile can be approximated by the equation,

$$Q \approx -P_{r_\parallel} v_p - n(m_e v_p^2)/2. \quad (1.2)$$

The above equation is valid even if the projectile undergoes Auger decays, since the electrons are associated with bound states in the projectile before their emission into the continuum. Therefore, the recoil momentum measured for a particular recoil-charge species is due to multielectron capture by the projectile. However, the above equation is not valid if ionization of the target occurs during the collision. In this case, the recoil-charge species is not due to electron capture by the projectile. Direct ionization of the target may become important in high velocity collisions above 1 a.u. For the collisional velocities studied in the experiment presented in this paper, the contribution due to direct ionization has been observed to be no bigger than a few percent [28,29]. Hence, errors due to measuring recoil-charge species produced by direct target ionization are small.

II. EXPERIMENT

The Xe^{30+} ions were produced in the cryogenic electron beam ion source (CRYEBIS) at the James R. Macdonald Laboratory at Kansas State University. This ion source is located on a 200 kV high voltage platform. The platform potential can be varied thus giving the experimenter a wide choice of energy for ion-atom collision experiments [30]. In this experiment, the platform voltage was varied to give a collisional velocity for the projectiles of 0.3 a.u. to 1.0 a.u.

The Xe^{30+} ions were extracted from the source, charge-to-mass analyzed by a 90° magnet, accelerated and delivered to the beamline with the target. The ion beam was collimated by use of two 4-jaw slits, the first just after the acceleration tubes and the second just before the switching magnet. The beam was further collimated by an 0.4 mm aperture upon enter into the chamber which contained the cold-gas-jet target. At the exit of this chamber, and no more than 15 cm from the entrance aperture was a 2 mm exit aperture. These entrance and exit aperture divide the entire beamline into three sections, the upstream, target, and downstream regions. The upstream and downstream regions were kept at pressures near 0.5×10^{-7} and 3×10^{-7} Torr, respectively, while the chamber which contained the target was kept at a background pressure of around 5×10^{-7} Torr. By limiting the length of the high pressure region which the projectiles had to traverse to a minimum, the amount of unwanted charge exchange occurring before and after the interaction region was kept to minimum. Also the three constraints, the two 4-jaw slits and entrance aperture, forced the projectile beam to propagate along the same trajectory for all collisional velocities.

Once the projectiles entered the target chamber, the collimated Xe^{30+} ion beam crossed a geometrically cooled gas-jet of Ar (see Fig. 1). The gas-jet target consisted of a capillary array separated by 10 mm from a 1 mm aperture into the target chamber. Target gas atoms with large transverse momentum components, with respect to the two geometrical apertures, never made it into the target chamber. This enabled us to produce an argon gas target with a momentum spread less than 2.0 a.u. along the projectile beam direction; the overall resolution including all contributions was measured to be 5.5 a.u.

The recoil ions were extracted by an electric field transverse to the projectile direction. During a single-collision event between Xe^{30+} and an atom, single-electron or multielectron transfer from the target to the projectile takes place. The collision leaves the argon target in a non-neutral state and the projectile in some excited

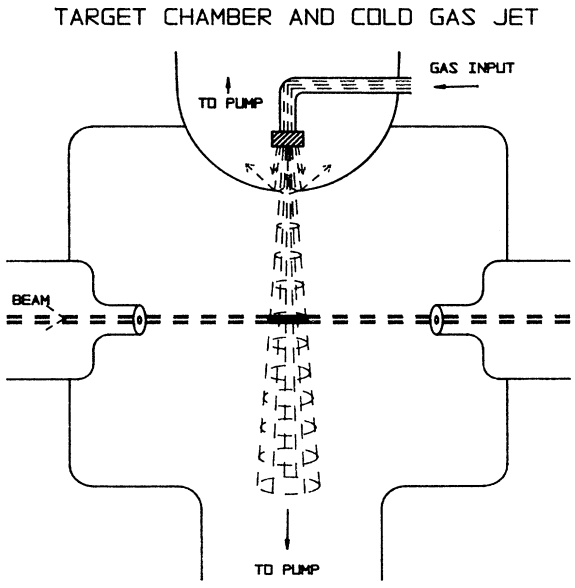

FIG. 1. The target chamber and cold-gas-jet assembly. Ar atoms with velocity components along the beam were prevented from reaching the projectile-target interaction region by a 1 mm aperture located 1 cm below the nozzle.

state. The electric field produced by the pusher assembly pushes this target recoil ion towards a two-dimensional position-sensitive detector where the record of both the position of the recoil on the detector and the time the recoil strikes the detector is measured. The projectile which is in some singly- or multiply-excited state relaxes either by photon or electron emission as it leaves the interaction region.

After the projectile enters the downstream section of the beamline, it encounters an electric field from a set of deflection plates and is then separated by charge state. At the end of the beamline is another two-dimensional (2D) position-sensitive detector which records both the time and position of the charge separated projectile signal. The timing signal from the projectile is compared with that from the recoil detector to produce a time-of-flight spectrum for the recoil ions. A schematic diagram showing both the experimental arrangement and geometry orientation of this experiment is shown in Fig. 2. Each individual time signal can also be plotted against the corresponding position signal on the projectile detector to produce a two-dimension plot which separates the final charge state of the projectile with the recoil ion charge state associated with that projectile (Fig. 3). In this two-dimensional coincidence spectra the separation of all possible charge exchange channels during the collision is accomplished. Further details of the technical aspects of the experiment are given in Ref. [31].

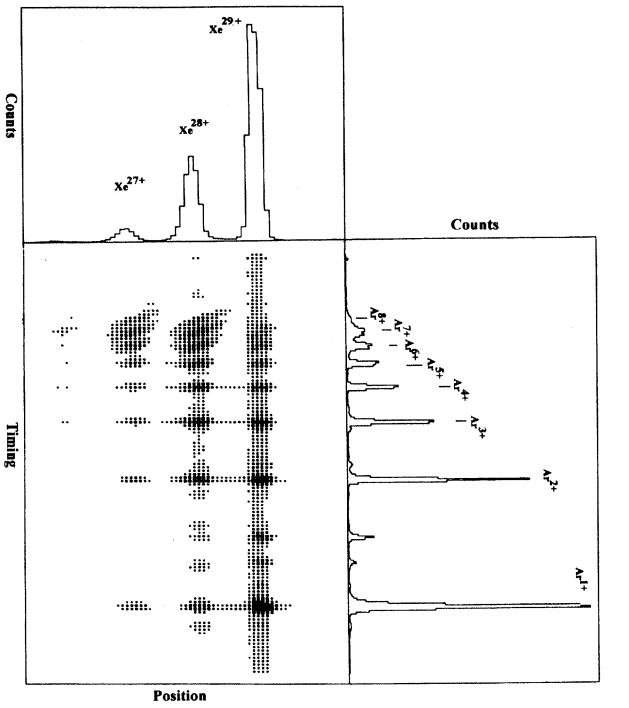

FIG. 3. A typical coincidence spectrum and its projections. The size of the dots in the 2D spectrum are proportional to the logarithmic intensity.

III. DATA ANALYSIS

As can be seen from Eq. (1.2), the Q value for a multielectron capture process is determined by the longitudinal momentum transferred, $P_{r_\parallel}$, the projectile velocity, v_p, and the number of electrons captured by the projectile, n. The number of electrons (n) captured by a projectile during a single-collisional event was obtained from the two-dimensional coincidence spectra under the assumption that the recoil ion charge state is completely determined by this primary capture. The longitudinal momentum transferred to the recoil ion is just $P_{r_\parallel} = m_r v_{r_\parallel}$. The longitudinal component of the velocity is related to the distance the recoil travels and time of flight of the ion to the detector. Since the time of flight and the final longitudinal position of the recoil ion was measured and recorded, the distance measurement reduced to the accurate knowledge of the initial longitudinal position, the zero position, where the recoil ion was created.

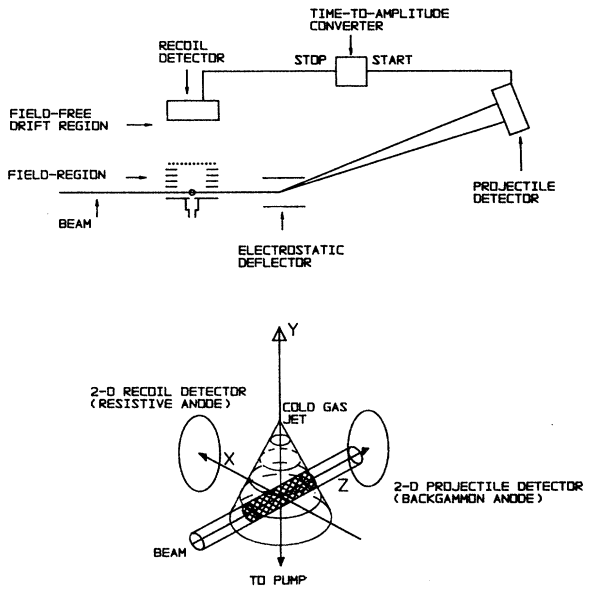

FIG. 2. Schematic of the experimental apparatus and the coordinate system used in the data analysis.

To measure accurately the final position on the detector for each recoil-charge state, events which were associated with a single recoil-charge species were isolated from the other charge species. The centroids of the longitudinal distribution of these events were then found. To determine the zero position of recoil ions on the detector, the resonant charge exchange reaction between He^+ projectile and a He target atom was used. By using a reaction of known Q value any stray electric fields within the target chamber which can effect the final recoil ion position measurement can be measured and corrected for. The position of the He^+ recoil ions on the recoil detector was measured as a function of pusher voltage and fit to the equation,

$$Z_{\text{final}} = Z_{\text{initial}} + a/\sqrt{V_{\text{pusher}}} + b/V_{\text{pusher}}. \qquad (3.1)$$

In the above equation, the term which is linear in

$1/\sqrt{V_{\text{pusher}}}$ is related to $v_{r_\parallel}$ of the reaction, whereas the term which is quadratic in $1/\sqrt{V_{\text{pusher}}}$ is related to any stray electric field along the beam direction. Since the Q value for resonant charge exchange is zero, the coefficient for the linear term was known and the zero position on the detector could be found. Thus all quantities, the constants Z_{initial} and b, and the variables Z_{final} and a for each recoil-charge species, were determined. From this $v_{r_\parallel}$, and ultimately the Q values for each capture channel and projectile velocity were calculated.

To determine the true number of events associated with each reaction channel, corrections due to random and background events, and "multiple-collisional" events were applied to the coincidence spectra. In the uncorrected coincidence spectra, different recoil-projectile coincidence channels were separated and the area and the number of events within these bins were recorded. To correct for random events, the area and number of events within a bin associated with a given projectile charge state but not any recoil-charge state was recorded. The random events were then scaled according to the area of each coincidence channel and subtracted from raw coincidence data. This produced a random and background corrected coincidence spectra. The correction for multiple-collision events followed the procedure described in Ref. [31].

IV. RESULTS AND DISCUSSION

The velocity dependence of the measured Q values for single-, double-, triple-, quadruple-, quintuple-, sextuple-, and septuple-electron capture is plotted in Fig. 4. Accompanying the experimental values of the Q values plotted in Fig. 4 are the MCBM predictions of these values for each of the capture channels. As can be observed from this figure, the measured Q values for single-electron and multielectron capture are velocity independent. Also, the MCBM predictions of these values agree with the measured experimental values. This model is based on the assumptions that projectile velocity is low (much less than an atomic unit of velocity), the energies of the captured electron are hydrogenic, and the electrons are independent. In the MCBM calculation, eight active, molecularized electrons were shared between the projectile and target. This produces a finite number of ways for the projectile to capture n electrons from these eight active electrons. Each channel for n electron capture has a different cross section, which is determined by the crossing radii and transfer probability specific to that channel. The calculated individual Q values for each of these channels are then weighted by the associated cross section to find the weighted average Q value for n electron capture. The MCBM predicts that the capture is occurring into a distribution of Rydberg projectile states ranging from an equivalent principal quantum number level 7 – 16. The agreement of the experimental Q values with the predictions of the weighted average from the MCBM model is striking.

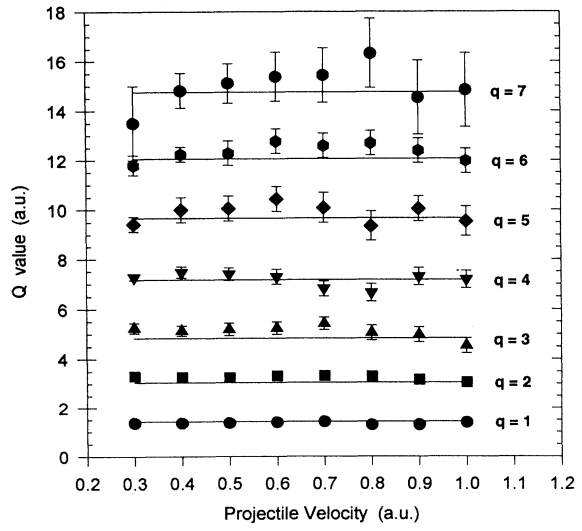

FIG. 4. Comparison of the experimentally measured Q values for single-, double-, triple-, quadruple-, quintuple-, sextuple-, and septuple-electron capture with the predictions from the MCBM for $Xe^{30+}+Ar \rightarrow Xe^{(30-q+n)+}+Ar^{q+}+ne^-$.

The error in the measured Q value is mainly due to the uncertainty in the location of the centroid of the longitudinal position of the recoil ion events on the detector and the uncertainty in the absolute location of the zero position for these ions. The errors associated with the measurement of single- through sextuple-electron capture are dominated by the uncertainty in the absolute zero. For increasing recoil-charge states the total number of events decreases. In the case for seven-electron capture, the limited number of counts for this channel coupled with both the uncertainty in the absolute zero point on the recoil detector and any inclusion of some six- and eight-electron capture events during the data analysis, lead to the larger error in the measurement.

The MCBM calculations shown in Fig. 4 do not allow target autoionization. In such a process the target produced from a single collision would be left in some multiexcited state which would then autoionize. This produces a measured recoil ion with a time of flight of an ion with the next higher charge state. However, the Q value associated with this measured recoil ion would be due to lower charge state. If this process were important, it would manifest itself by lowering the Q value below that which would occur in the absence of this process. This effect is not observed, and we, therefore, conclude that target autoionization is unlikely to be playing a large role in these collisions.

The velocity dependence of the recoil-charge state distribution is shown in Figs. 5 and 6. For the first three charge states of the recoil, no measurable reduction or increase in their production occurs in this velocity range. However, for the higher recoil-charge states, both increases and decreases in their production are observed in the data suggesting that collisional dynamics are beginning to play a more important role in their production as the collisional velocity increases. In Fig. 7 we compare the experimentally averaged data for recoil production above and below 0.55 a.u. collisional velocity with the

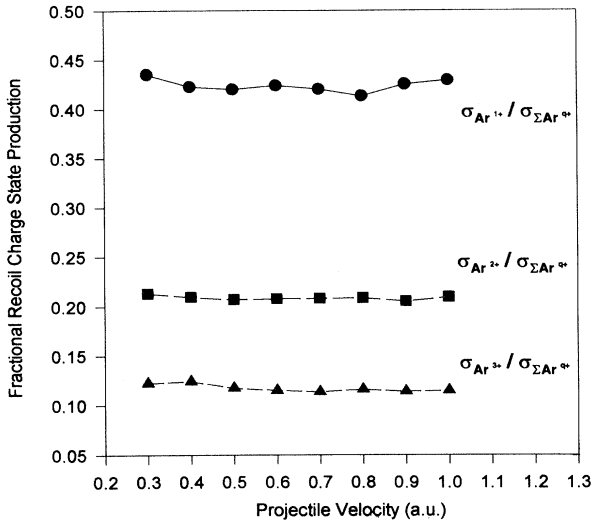

FIG. 5. Velocity dependence of the recoil-charge state fraction productions for Ar^{1+}, Ar^{2+}, and Ar^{3+}.

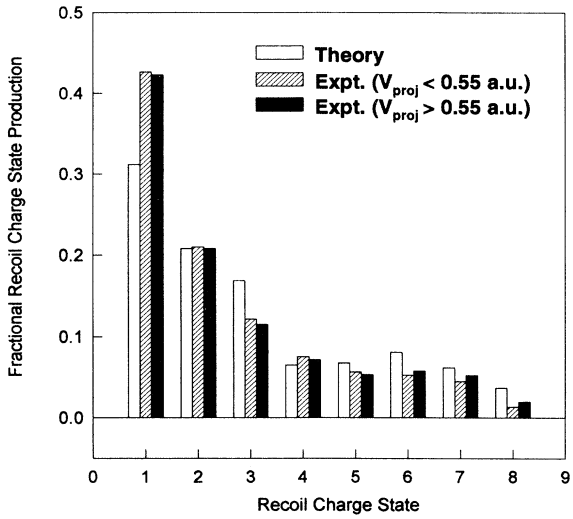

FIG. 7. Comparison of the experimentally averaged data of the recoil production fractions with the theoretical predictions of the MCBM.

predictions of the MCBM. While the general agreement is good, the MCBM slightly underestimates the production of the single charged recoils and tends to overestimate the production of the higher recoil-charge states for both velocity ranges.

In Fig. 8, the velocity dependence of the production of charge changing projectiles is shown. As can be observed from the figure, at these collisional velocities around 70% of the total capture flux is directed in single-electron retention, while two-electron retention and three-electron retention are around 25% and 0.5%, respectively. Four-electron retention by the projectile is less than a tenth of the three-electron retention and, therefore, is a negligible fraction of the total charge changing flux. The retention distribution is for the most part velocity independent with a possibility of a slight decrease in the single-electron retention channel and a subsequent increase in the two-electron retention channel. Coupling this with the charge state distribution of the recoils, we observe that most of the multielectron capture flux is reemitted into the projectile continuum. This is not surprising since the MCBM predicts capture into excited states well above the ground state of the projectile.

Since all charge changing channels are experimentally separated in the reduced coincidence spectra, the separation of the single and multiple Auger channels within any given recoil species is accomplished for recoil-charge states greater than one. For each of these recoils species the percentage of each decay channel in the total flux can be plotted as a function of collisional velocity. Figures 9–11 show this plot for recoil-charge state species two,

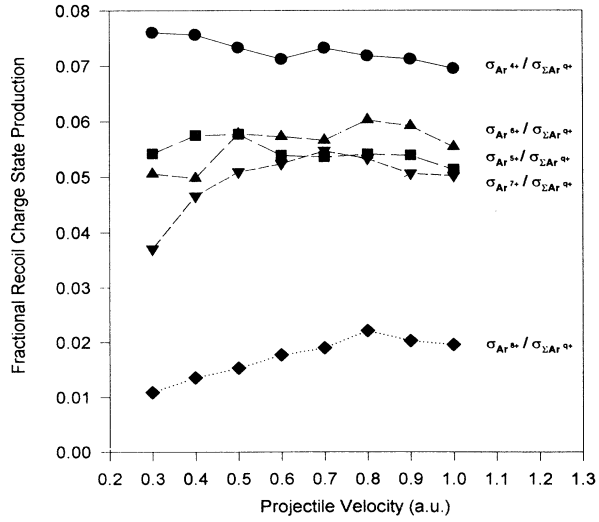

FIG. 6. Similar to Fig. 5, for Ar^{4+}, Ar^{5+}, Ar^{6+}, Ar^{7+}, and Ar^{8+}.

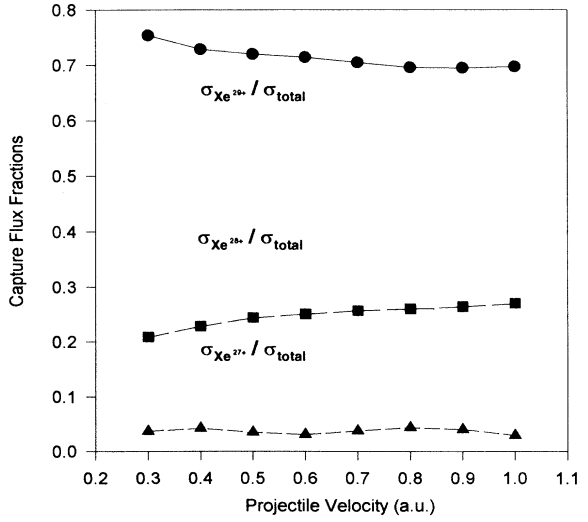

FIG. 8. Velocity dependence for the production of the charge changing projectiles.

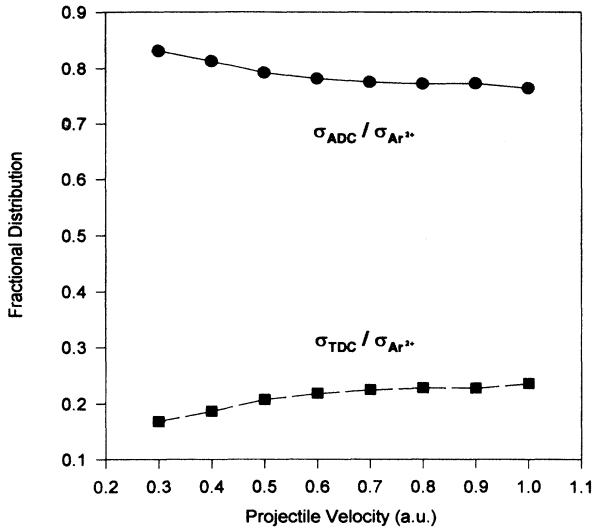

FIG. 9. Velocity dependence of the capture-decay channels of the projectiles associated with production of Ar^{2+}, double-electron capture (DC): autoionizing double capture (ADC) and true double capture (TDC).

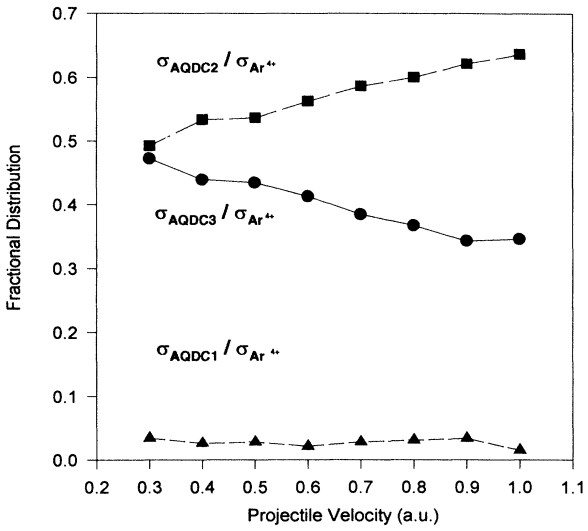

FIG. 11. Similar to Fig. 9, for the production of Ar^{4+}, quadruple electron capture (QDC): autoionizing quadruple capture with three Auger decays (AQDC3), autoionizing quadruple capture with two Auger decays (AQDC2), and autoionizing quadruple capture with one Auger decay (AQDC1).

three, and four. While the average Q value is nearly velocity independent, subtle variations with velocity in the (n, l) population distribution nevertheless occur. These are revealed in the velocity dependence of the relative probabilities for radiative and nonradiative stabilization in the various outgoing channels. In all cases in Figs. 9–11, the probability of retaining more than two electrons is quite small. We focus our attention on the competition between the radiative and nonradiative decay of the two-electron system which is either produced directly (in double capture) or from Auger decay following the capture of three or four electrons. First, we note that the

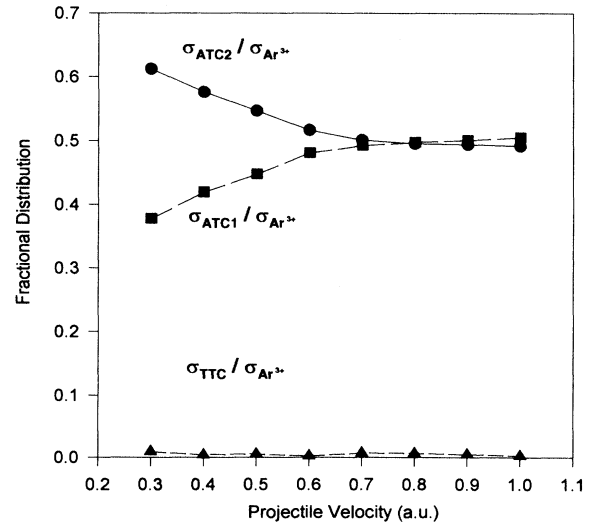

FIG. 10. Similar to Fig. 9, for the production of Ar^{3+}, triple-electron capture (TC): autoionizing triple capture with two Auger decays (ATC2), autoionizing triple capture with one Auger decay (ATC1), and true triple capture (TTC).

radiative stabilization of configurations fed via Auger cascades is much greater than that for those fed directly, e.g., $\sigma_{\mathrm{AQDC2}}/\sigma_{\mathrm{Ar}^{4+}} > \sigma_{\mathrm{ATC1}}/\sigma_{\mathrm{Ar}^{3+}} > \sigma_{\mathrm{TDC}}/\sigma_{\mathrm{Ar}^{2+}}$, where σ_{AQDC2} is the cross section for autoionizing quadrupole capture with two Auger decays, σ_{ATC1} is the cross section for autoionizing triple capture with one Auger decay, and σ_{TDC} is the cross section for true double capture. This is probably due to the fact that the Auger decay of a triply excited configuration is more likely to feed a doubly-excited state with very different (n, n') than would a direct double capture. Second, we note that the probabilities for radiative stabilization of any two-electron configurations $(\sigma_{\mathrm{TDC}}/\sigma_{\mathrm{Ar}^{2+}}, \sigma_{\mathrm{ATC1}}/\sigma_{\mathrm{Ar}^{3+}}, \sigma_{\mathrm{AQDC2}}/\sigma_{\mathrm{Ar}^{4+}})$ increase slowly with velocity.

To describe the observed distribution of the decay channels in the projectile-recoil coincidence spectrum, accurate knowledge of transition rates, branching ratios, population distributions, and energy levels of multielectron configurations in successive ionization states in the projectile is required. In the absence of information at this level of detail, we suggest a more general interpretation of the observed velocity dependence. The absence of any dependence of the Q values or relative cross sections on projectile velocity suggests that the final n distributions predicated by the MCBM are correct. However, as the collision velocity is raised, more angular momentum is brought into the collision. For a given transition radius R, characteristic of populating a particular final n, the product mvR increases with v. Such a trend is well established previously [24,25,32,33]. Generally, the larger the l of the transferred electrons, the smaller the probability for decay by autoionization [34]. Therefore, as the angular momentum of the individual electron increases within any manifold, the total Auger rate within the manifold would tend to decrease in favor of radiative

stabilization. This decrease in the Auger rate is observed in the double-electron coincidence channels.

V. SUMMARY AND CONCLUSIONS

In this paper, we have presented the measurements of Q values using longitudinal momentum recoil spectroscopy for single-electron and multielectron transfer during a single collision between a Xe^{30+} projectile with a Argon target. We have used a cold gas jet to produce a target with a momentum spread of less than 2 a.u. of longitudinal momentum. This single-electron and multielectron transfer process was studied at collisional velocities ranging from 0.3 a.u. to 1.0 a.u.

From the invariance of the measured Q values over the collisional velocity range studied and comparison with the MCBM weighted Q predictions which are velocity independent, we can draw the following conclusions. The distribution of the captured electrons into different excited state n manifolds is not changing. However, there seems to be evidence for a redistribution to larger l within the given manifold with increasing velocity. The MCBM predictions of the Q value are valid in the collisional velocity regions where single-electron and multielectron capture dominates the ion-atom collision interaction.

Looking at the production of single- and double-electron retention as the collisional velocity increases, there is a slight decrease in single-electron retention and a slight increase in double-electron retention. Three-electron retention is a small fraction of the total projectile charge changing flux. Similarly looking at the production of recoil species, in coincidence with the final charge changing projectile species, we have seen an increase in two-electron retention at the expense of one-electron retention for double-, triple-, and quadruple-electron capture. These velocity dependences are possibly due to an increase in the average angular momentum of the captured electrons populated within a given n manifold as the collisional velocity increases, forming configurations which tend to stabilize radiatively over autoionization. Upon comparisons with the predictions with the MCBM, single-electron capture is slightly underestimated by the model, but the general distributions of the higher recoil-charge states are reproduced. Single-electron capture accounts for around 45% of the total charge changing projectile flux while double-electron capture accounts for 30% and triple- through octuple-electron capture accounts for about 25%.

Overall, the MCBM does well at accounting for both the Q values and relative intensities observed for this highly-charged projectile. Since the basic assumptions of the model are better satisfied for higher projectile charge, and the final projectile state densities are smoother, it is not surprising that a model which does not pretend to be sensitive to details of specific couplings and level placements should have its greatest successes for the highest projectile charge. Perhaps less obvious is that the model remains successful over a fair range in projectile velocity, up to 1 a.u., for such case. The only velocity dependent effects observed in this velocity range may be due to changing final distributions about which the model has nothing to say.

ACKNOWLEDGMENTS

This work was supported by the Division of Chemical Sciences, Office of Basic Energy Research, U.S. Department of Energy.

[1] R. Mann, C. L. Cocke, A. S. Schlachter, M. Prior, and R. Marrus, Phys. Rev. Lett. **49**, 1329 (1982).
[2] S. Ohtani, Y. Kaneko, M. Kimura, N. Kobayashi, T. Iwai, A. Matsumoto, K. Okuno, S. Takagi, H. Tawara, and S. Tsurubuchi. J. Phys. B **15**, L525 (1982).
[3] C. Schmeisssner, C. L. Cocke, R. Mann, and W. Meyerhof, Phys. Rev. A **30**, 1661 (1984).
[4] B. A. Huber, H.-J. Kahlert, and K. Wiesemann, J. Phys. B **17**, 2883 (1984).
[5] E. H. Nielsen, L. H. Andersen, A. Bárány, H. Cederquist, J. Heinemeier, P. Hvelplund, H. Knudsen, K. B. MacAdam, and J. Sorensen, J. Phys. B **18**, 1789 (1985).
[6] H. Cederquist, L. H. Andersen, A. Bárány, P. Hvelplund, H. Knudsen, E. H. Nielsen, J. O. K. Petersen, and J. Sorensen, J. Phys. B **18**, 3951 (1985).
[7] J. P. Giese, C. L. Cocke, W. Waggoner, L. N. Tunnell, and S. L. Varghese, Phys. Rev. A **34**, 3770 (1986).
[8] R. W. McCullough, S. M. Wilson, and H. B. Gilbody, J. Phys. B **20**, 2031 (1987).
[9] E. Y. Kamber, C. L. Cocke, J. P. Giese, J. O. K. Petersen, and W. Waggoner, Phys. Rev. A **36**, 5575 (1987).
[10] S. M. Wilson, R. W. McCullough, and H. B. Gilbody, J. Phys. B **21**, 1027 (1988).
[11] E. Y. Kamber, Nucl. Instrum. Methods Phys. Res. Sect. B **40/41**, 13 (1989).
[12] H. Cederquist, L. Liljeby, C. Biedermann, J. C. Levin, H. Rothard, K. O. Groeneveld, C. R. Vane, and I. A. Sellin, Phys. Rev. A **39**, 4308 (1989).
[13] C. Biedermann, H. Cederquist, L. R. Andersen, J. C. Levin, R. T. Short, S. B. Elston, J. P. Gibbons, H. Anderson, L. Liljeby, and I. A. Sellin, Phys. Rev. A **41**, 5889 (1990).
[14] P. Roncin, M. N. Gaboriaud, and M. Barat, Europhys. Lett. **16**, 551 (1991).
[15] C. L. Cocke and R. E. Olson, Phys. Rep. **205**, 153 (1991).
[16] H. Lebius and B. A. Huber, Z. Phys. D **23**, 61 (1992).
[17] H. Schmidt-Böcking *et al.*, in *Proceedings of the Seventeenth International Conference on the Physics of Electronic and Atomic Collisions, Brisbane, 1991*, edited by W. R. MacGillvray, I. E. McCarthy, and M. C. Standage (AIP, New York, 1992).
[18] R. Ali, V. Frohne, C. L. Cocke, M. P. Stökli, S. Cheng, and M. L. A. Raphaelian, Phys. Rev. Lett. **69**, 2491 (1992).
[19] V. Frohne, S. Cheng, R. Ali, M. Raphaelian, C. L. Cocke, and R. E. Olsen, Phys. Rev. Lett. **71**, 696 (1993).

[20] W. Wu, J. P. Giese, I. Ben-Itzhak, C. L. Cocke, P. Richard, M. P. Stöckli, R. Ali, H. Schöne, and R. E. Olson, Phys. Rev. A **48**, 3617 (1993).
[21] H. Ryufuku, K. Sasaki, and T. Watanabe, Phys. Rev. A, **21**, 745 (1980).
[22] A. Bárány, G. Astner, H. Cederquist, H. Danared, S. Huldt, P. Hvelplund, A. Johnson, H. Knudsen, L. Liljeby, and K. G. Rensfelt, Nucl. Instrum. Methods Phys. Res. Sect. B **9**, 397 (1985).
[23] A. Niehaus, J. Phys. B **19**, 2925 (1986).
[24] M. L. A. Raphaelian, H. G. Berry, N. Berrah, and D. Schneider, Phys. Rev. A **48**, 1292 (1993).
[25] Z. Chen and C. D. Lin, Phys. Rev. A **48**, 1298 (1993).
[26] J. H. Posthumus, P. Lukey, and R. Morgenstern, J. Phys. B **25**, 987 (1992).
[27] R. Ali, C. L. Cocke, M. L. A. Raphaelian, and M. P. Stöckli, J. Phys. B **26**, L685 (1993).
[28] H. Cederquist, C. Biedermann, N. Selberg, E. Beebe, M. Pajek, and A. Bárány, Phys. Rev. A **47**, R4551 (1993).
[29] W. Wu (private communication).
[30] M. P. Stöckli, R. M. Ali, C. L. Cocke, M. L. A. Raphaelian, P. Richard, and T. N. Tipping, Rev. Sci. Instrum. **63**, 2822 (1992).
[31] R. Ali, C. L. Cocke, M. L. A. Raphaelian, and M. Stockli, Phys. Rev. A **49**, 3586 (1994).
[32] D. Dijkkamp, C. Ćirić, E. Vlieg, A. de Boer, and F.J. de Heer, J. Phys. B **25**, 4763 (1985).
[33] J. P. M. Beijers, R. Hoekstra, R. Morgenstern, Phys. Rev. A **49**, 363 (1994).
[34] Robert D. Cowan, *The Theory of Atomic Structure and Spectra* (University of California Press, Berkeley, 1981), pp. 549–563.